

Large-Volume Plasma Device with Internally Mounted Face-Type Planar Microwave Launchers for Low-Temperature Sterilization

Mrityunjai Kumar Singh¹ & Masaaki Nagatsu^{2,*}

¹Indian Agricultural Research Institute, Regional Station-Karnal 132001, India; ²Graduate School of Science and Technology, Shizuoka University, 3-5-1, Johoku, Naka-ku, Hamamatsu 432-8561, Japan

*Address all correspondence to: Masaaki Nagatsu, 3-5-1, Johoku, Naka-ku, Hamamatsu 432 8561, Japan; Tel.: +81-53-478-1081; tmnagat@ipc.shizuoka.ac.jp

ABSTRACT: In this study, large-volume microwave excited surface-wave and volume-wave plasmas were investigated for low temperature sterilization of medical instrument. The two planar microwave launchers, each supported by a 1.5-kW magnetron, were face-to-face installed inside the vacuum chamber of plasma device for homogeneous sterilization. The spatial distributions of plasma discharges in the surface-wave and volume-wave modes were characterized under various discharge conditions using single or double microwave launchers of the experimental setup. The electron density increased to about twice in the case of double launchers as compared to single launcher without any microwave interference between two launchers. With this plasma setup, we confirmed the successful inactivation of Tyvek-wrapped spore-forming bacteria at temperatures less than 70°C and within 70 to 80 min with time-modulated surface-wave and volume-wave plasma, respectively.

KEY WORDS: plasma sterilization, surface-wave plasma, volume-wave plasma, spore-forming bacteria

I. INTRODUCTION

An increasing number of researchers are investigating low-cost techniques to sterilize medical instruments at low temperatures. Such methods could also be widely applied for hygiene maintenance in the food industry. Although there are many available techniques for sterilization based on thermal treatment (e.g., dry heat, steam autoclave), chemical treatment (e.g., ethylene oxide, hydrogen peroxide), and exposure to radiation (e.g., X-rays, gamma radiation), all these conventional methods for processing are limited by their own merits and demerits. Plasma sterilization techniques are a novel alternative to available techniques, because materials can be processed at low temperatures in a short period of time, and there are potentially no toxic effects. Different types of low pressure^{1–19} and atmospheric pressure^{20–25} discharges can be used for sterilization. Atmospheric pressure plasmas have a great advantage because no pumping system is required. However, this technology is still being developed so that it can be used to sterilize items with large areas, such as three-dimensional medical devices. The large area plasma sources suitable for sterilization are indispensable in the medical industry to taper off the loading effect.

Because of the complex geometry of medical devices, their sterilization requires

a homogeneous plasma source, in which all surfaces of an instrument are sufficiently exposed to the sterilizing agents, such as reactive species of ions, atoms, and vacuum ultraviolet (VUV)/UV photons produced by plasma. Apart from homogeneity, practical applications of plasma sterilization are also required to sterilize medical instruments inside perforated resinous packages, such as Tyvek used for sterile packaging, so that their safe use can be ensured at a later date. Presently the surface-wave plasma (SWP), which is an over-dense plasma (electron density $n_e > 3.5 \times 10^{11} \text{ cm}^{-3}$) produced by high frequency waves such as microwaves, is one of the reliable and suitable plasma sources for low temperature, high density plasma processing at low to moderate pressures. Other studies have already demonstrated that enlarged SWP satisfies the requirements for processing compact items with large areas.^{26–28} These planar surface-wave plasmas can provide highly efficient power transfer from the generator to the plasma over a large range of operating conditions without the use of electrodes.²⁹ This characteristics of SWPs are very useful for various applications in the fabrication of electronic materials, such as ultra-large-scale integrations and liquid crystal display panel manufacturing. SWPs also have other industrial applications, such as medical sterilization, where spatial uniformity of the large area plasma source apart from high density plasma is required for fast processing.

In this paper, we present the experimental results on characterization and sterilization applications of the large-volume, 2.45-GHz microwave excited plasma device consisting of two internally installed face-type planar launchers. In addition to the SWP, the volume-wave plasma (VWP), which has a lower electron density than the cutoff density of $n_e = 7.0 \times 10^{10} \text{ cm}^{-3}$, was also produced over the chamber volume under specific discharge conditions with this setup. The three-dimensional distribution of the plasma parameters were investigated with a Langmuir probe. The sterilization characteristics of directly exposed *Geobacillus stearothermophilus* spores were also investigated for both surface-wave and volume-wave plasmas.

II. EXPERIMENT

A. Experimental Setup

Figure 1 shows the schematic drawings of the experimental setup. The discharge chamber dimensions were 520 mm in length, 514 mm in width, and 555.5 mm in height. The circular metal turntable with a diameter of 400 mm was located below the chamber at a distance between the turntable, and the central axis between the two launchers, h , is 250 mm. Two microwave launchers with a diameter of 470 mm were face-to-face installed with a distance of $d = 450$ mm inside the chamber. The microwave launchers consisted of a coaxial waveguide and cylindrical planar cavity in which a quartz dielectric plate with a diameter of 420 and thickness of 15 mm was fixed with screws on the stainless steel housing of launcher. The present microwave launchers overcome the problem of a thick dielectric plate to maintain vacuum, because vacuum was held only at small area with a diameter of roughly 50 mm.^{27,28} A schematic drawing of the microwave launcher

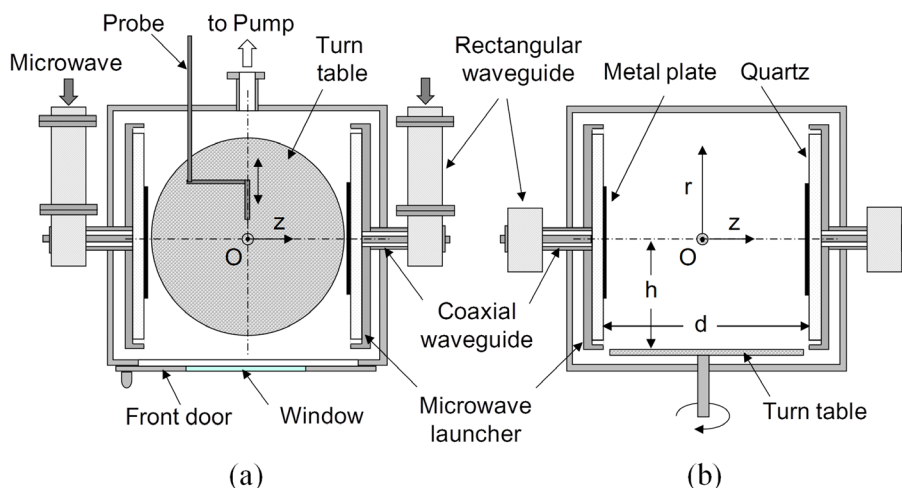


FIG. 1: Schematic drawings of the experimental setup chamber; (a) top view, and (b) front view

is shown in Fig. 2. At the front side of the planar microwave launcher, a 200-mm diameter thin metal plate was attached in the center of the quartz surface to prevent direct microwave propagation toward the vacuum chamber. Thus, microwaves were launched from the ring shape of quartz surface. Additionally, there was a gap of 5 mm between the microwave launcher housing and the periphery of quartz plate, which served as the microwave antenna in the VWP production. Productions of the large volume SWP and VWP with a similar type of microwave launchers have been already demonstrated and is presented in previous studies.^{27,28}

Microwaves at a frequency of 2.45 GHz guided through a rectangular waveguide

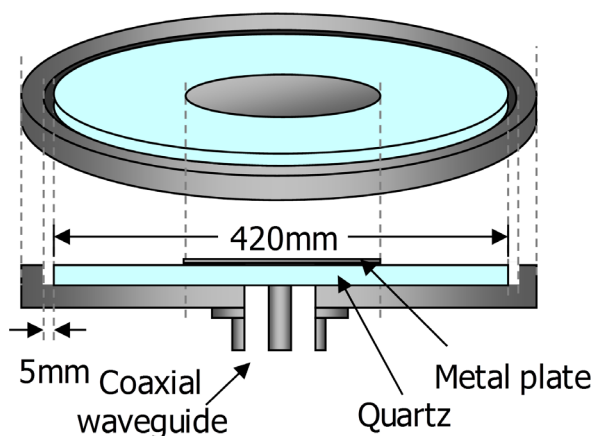


FIG. 2: Schematic drawing of planar microwave launcher having metal plate attached centrally to the quartz surface

are converted into a coaxial waveguide mode and then transferred to the microwave planar launchers. The incident microwave power can be varied from 0.2 kW to 1.5 kW, the maximum power supply from each magnetron generator. The reflected microwave power was minimized to almost zero by adjusting the E-H tuners installed for impedance matching between the plasma and microwave circuit. The working gases were fed into the discharge chamber through a mass flow controller after evacuation. The chamber pressure was reduced to roughly 1 Pa by rotary and Roots pump system within 2 min.

As shown in Fig. 1, a homemade Langmuir probe system was inserted for measuring plasma parameters. It was also used as a monopole antenna probe to monitor the microwave electric field to check whether it was in SWP or VWP mode, because the microwaves were perfectly absorbed by the plasma in SWP mode and not in VWP mode. The Langmuir probe was made of a platinum wire, 0.6 mm in diameter and 6.0 mm long. The probe was shielded with a stainless steel pipe with an outer diameter of 6 mm, excluding the wire tip part. The probe tip was scanned horizontally through the port mounted on the chamber sidewall. The electron density was determined from the ion saturation current of the probe, and electron temperature was deduced from the slope of probe characteristics. The VWP characteristics were measured with a double probe made of platinum wire 0.7 mm in diameter and 9.5 mm long, because it was possible that the VWP was produced in isolation from the chamber wall.

The optical emission spectroscopy (OES) of the plasma discharges was performed with an Acton SpectraPro 2300i monochromator (Princeton Instruments Inc.). The observable spectrum range was 200–800 nm, and typical spectra were measured with an integration time of 100 msec. The emission spectra were measured at the central position of the side glass window (Fig. 1) of the experimental setup, collecting light with an optical fiber directed perpendicularly to this window.

B. Plasma Parameters

The plasma parameters, electron density and electron temperature, which describe the discharge characteristics, were measured at radial and axial axis of the chamber. These characteristics were measured at different incident powers and pressures of the working gases of Ar, He, and air-simulated N_2/O_2 mixture gas. The plasma characteristics with noble gases Ar and He were determined primarily to ascertain the stable and uniform discharges in SWP and VWP modes, respectively. The air-simulated gas was also studied because air may be used as an inactivating gas in future plasma sterilizations.

The temperature of objects to be sterilized is an important parameter to prevent the thermal damage of wrapping resin material. We measured the temperature in various sterilization experiments by placing thermo-label sheets (Nichiyu, Thermo Label 5E-50, 5E-75 and 5E-100) just below the spore samples. The color change from white to black of the thermo-sensitive dots indicated the temperature during the experiment.

C. Biological Procedure

The sterilization experiments were performed using directly exposed *Geobacillus stearothermophilus* (ATCC 12980, Raven Biological) spores as the sterility indicator. The spores were pasted on oblong polished stainless steel discs with a spore population of $1.9\text{--}3.4 \times 10^6$. After plasma treatment, samples were properly washed and vortexed with 1.5 mL of brain-heart infusion (BHI) solution in the test tube. After an appropriate dilution, 0.1 mL of the spore suspension was inoculated onto nutrient agar media and incubated for two days at 55°C and then the grown colony-forming units (CFUs), each representing a surviving cell, were counted. The reduction in the number of CFUs from treated samples plotted against plasma treatment times, so-called survival curves, were compared with untreated spore samples. To record the changes in the morphological structures caused by plasma irradiation, the untreated and treated spores pasted on stainless steel discs were coated with a 20-nm thin film of evaporated gold and then observed with scanning electron microscopy (JEOL, JSM-6360) at a typical accelerating voltage of 15 kV.

III. RESULTS AND DISCUSSION

A. Discharge Characterization

The input microwave power dependencies of the plasma discharges sustained in Ar and air-simulated N_2/O_2 mixture gas SWPs at different pressures are shown in Fig. 3. Here, the Langmuir probe was fixed at $r = 0$ and $z = 22.5$ cm (central position). We regard the net microwave power simply as the reflected power subtracted from the incident power. Figures 3(a) and (b) show the ion saturation currents measured at a biasing voltage of -30 V versus net microwave power at pressures of 10.5 Pa and 20.5 Pa in the case of Ar plasmas and 12.5 and 23.5 Pa in air-simulated N_2/O_2 mixture gas plasmas, respectively. It is noted that the ion saturation currents monotonically increased with the incident microwave power without any density jump in both conditions. The ion saturation currents at $z = 22.5$ cm decreased as pressure increased because the plasma localization near the quartz plate has a shorter mean free path at a higher pressure.

Figures 4(a) and (b) show that radial distributions of electron density in Ar plasma with a single launcher at 790 W and 1440 W and double launchers at 1480 W. The distributions are quite analogous for almost the same net input power at 1440 W in the case of single launcher and 1480 W for double launchers. The results of these experiments indicate that the microwave power was almost absorbed by the high density plasma in the front of launchers, so there was no interference between the two microwave systems.

Fig. 5 shows the radial spatial distributions of the ion saturation currents in the SWPs at powers of 1.5 kW and 3.0 kW with Ar and air-simulated N_2/O_2 gas at 12.5 Pa using the double launcher mode. It is obvious from these results that the large-volume plasmas were produced over a wide area spreading to the vacuum chamber wall. Moreover, we found that ion saturation currents were doubled with doubled incident power

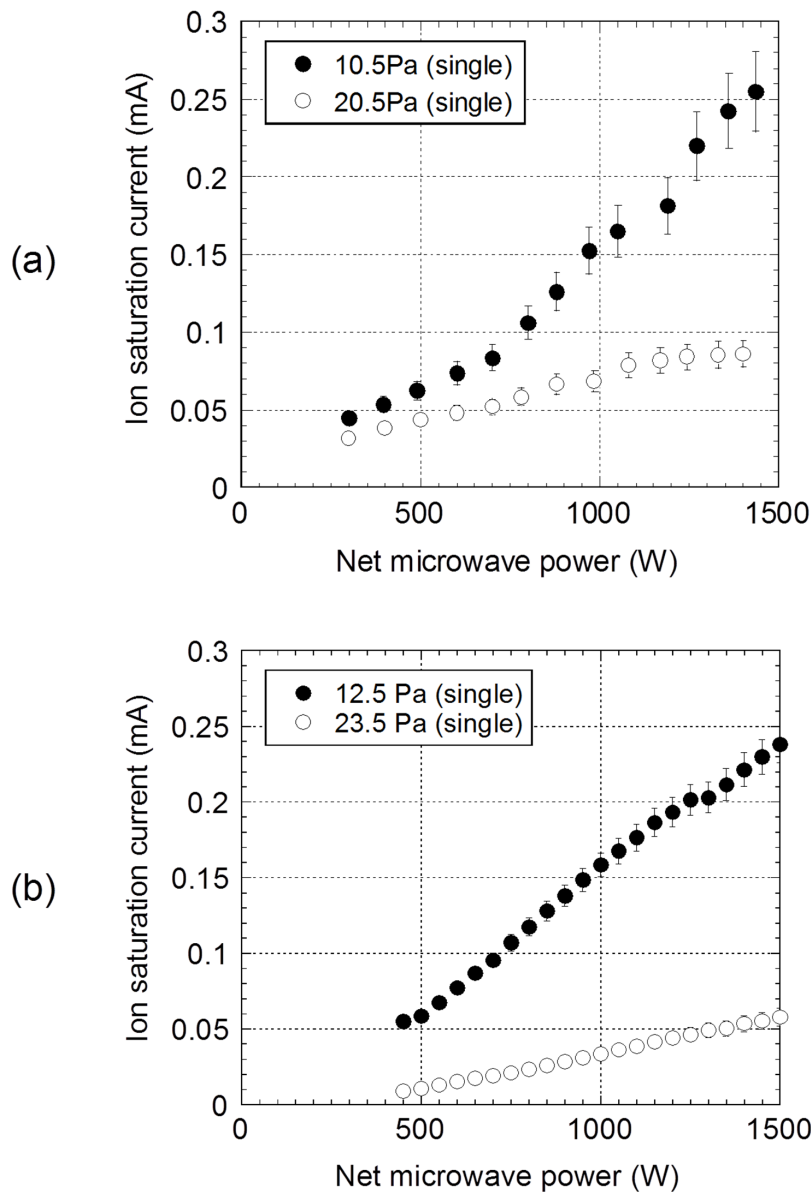


FIG. 3: Incident power dependencies of ion saturation currents at various pressures using single launcher (a) Ar plasma at 10.5 and 20.5 Pa, and (b) air-simulated N₂/O₂ mixture gas plasma at 12.5 and 23.5 Pa

for both Ar and air-simulated gases. This also confirms that microwaves didn't interfere with each other when the double launchers were used, and spatial distributions of ion saturation currents were roughly superimposed.

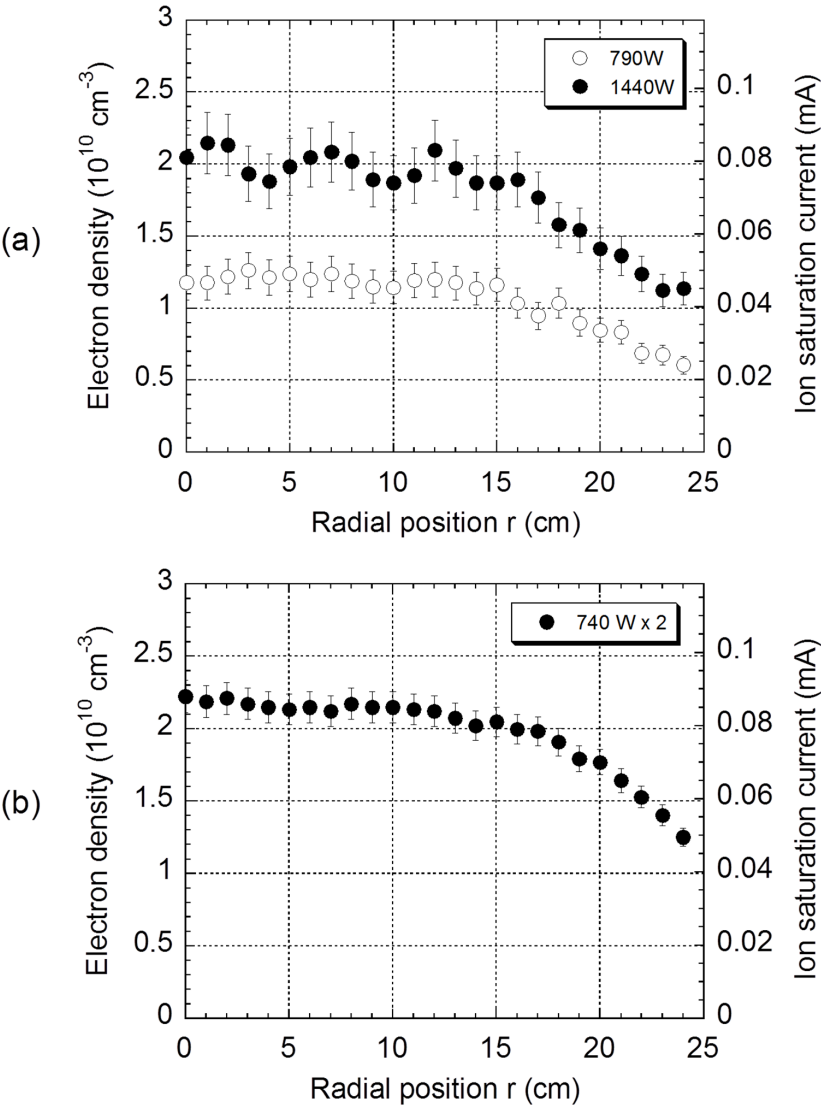


FIG. 4: Radial distributions of electron density in Ar plasma with (a) single launcher at 790 and 1440 W and (b) double launchers at 1480 W

The radial distributions of electron temperature in the SWPs with Ar gas and air-simulated N_2/O_2 mixture at 12.5 Pa for single (1 kW) and double launcher (2 kW) modes are shown in Fig. 6. The electron temperatures were roughly 1.0 to 1.3 eV when the operating parameters of the single launcher were 1 kW and 1.2 to 1.5 eV and when the double launchers had a total power of 2 kW, respectively, and no significant variations were observed when power was increased.

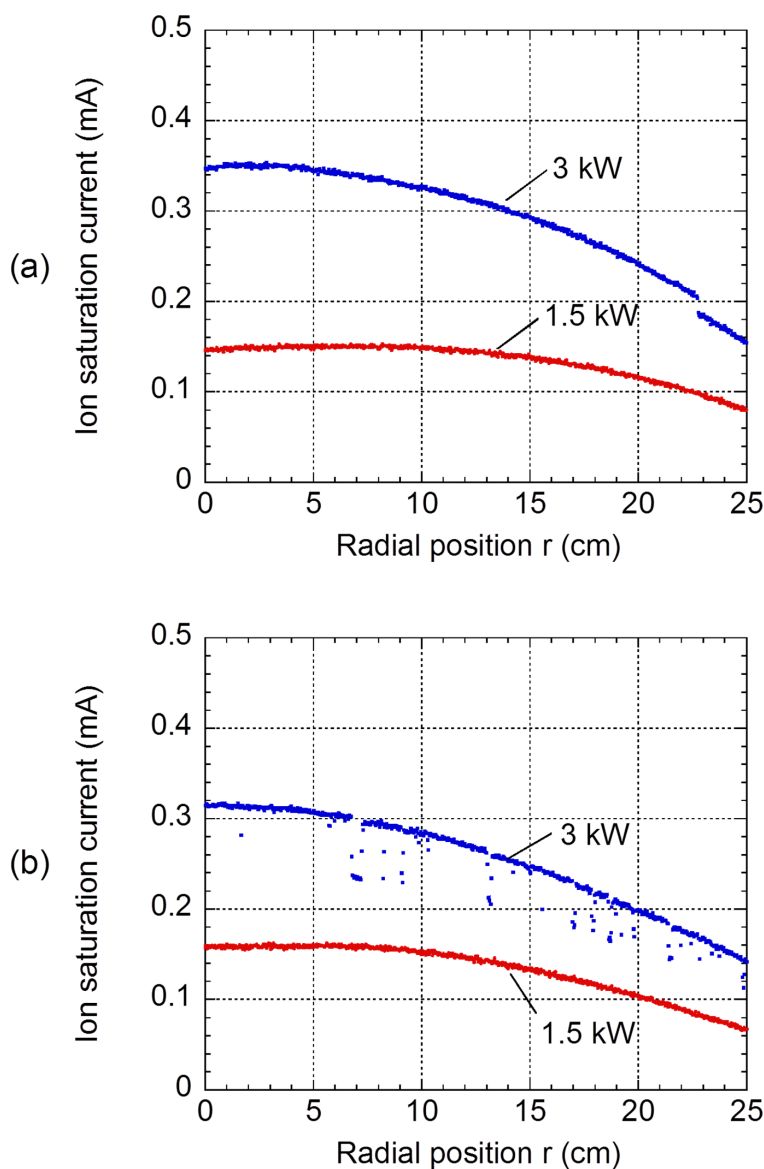


FIG. 5: Radial spatial distributions of the ion saturation currents in the SWPs at power of 1.5 and 3.0 kW with (a) Ar and (b) air-simulated N_2/O_2 mixture gas at 12.5 Pa using double launcher mode, respectively

In the present experimental setup, we demonstrated the discharge transition from VWP to SWP mode in He gas plasma under various discharge conditions of microwave power and pressure, as shown in Fig. 7(a). Electric fields were detected by a monopole antenna probe inside the chamber while in the VWP mode, whereas no electric fields

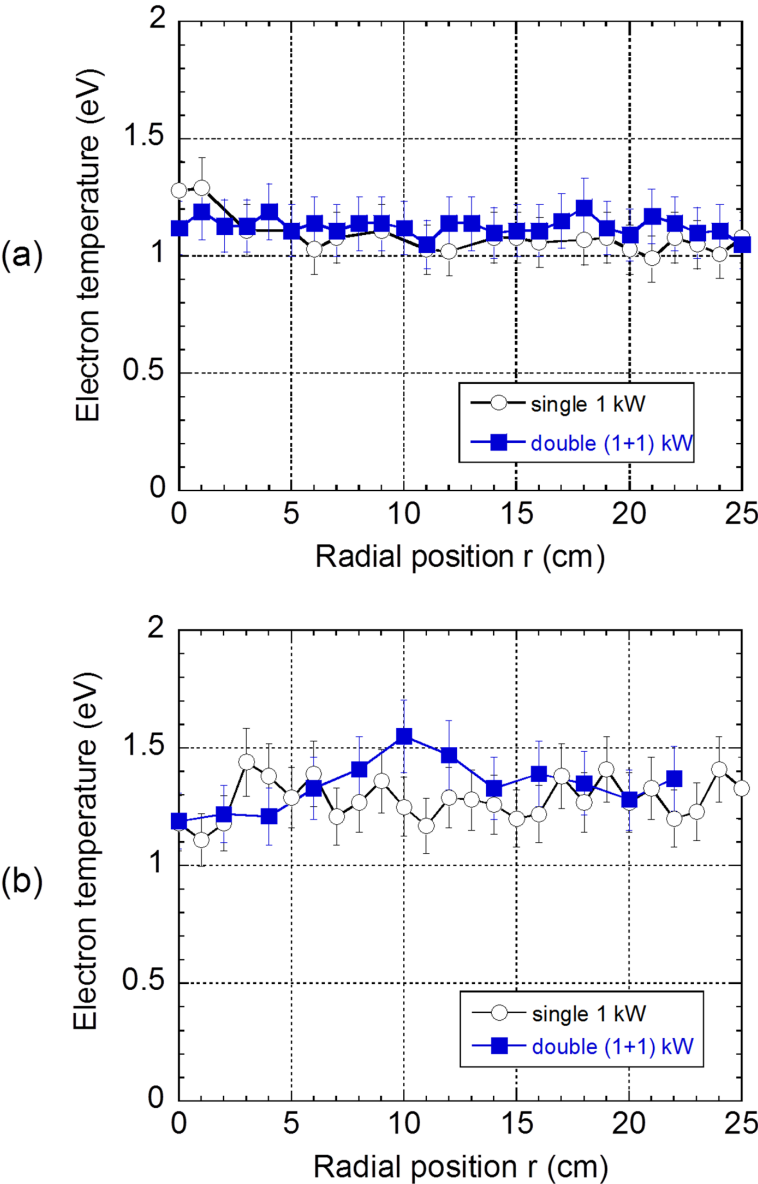


FIG. 6: Radial distributions of electron temperature in the SWPs with (a)Ar gas and (b) air-simulated N_2/O_2 mixture at 12.5 Pa for single (1 kW) and double launcher (2 kW) modes, respectively.

were detected in SWP mode. These results are similar to previous findings.²⁷ When the incident power was increased at the same pressure, a bright discharge was produced near the quartz plate of the launcher (i.e., SWP), as shown in Fig. 7(b). On the other hand, when incident power was decreased to certain values at the same pressure, the discharge

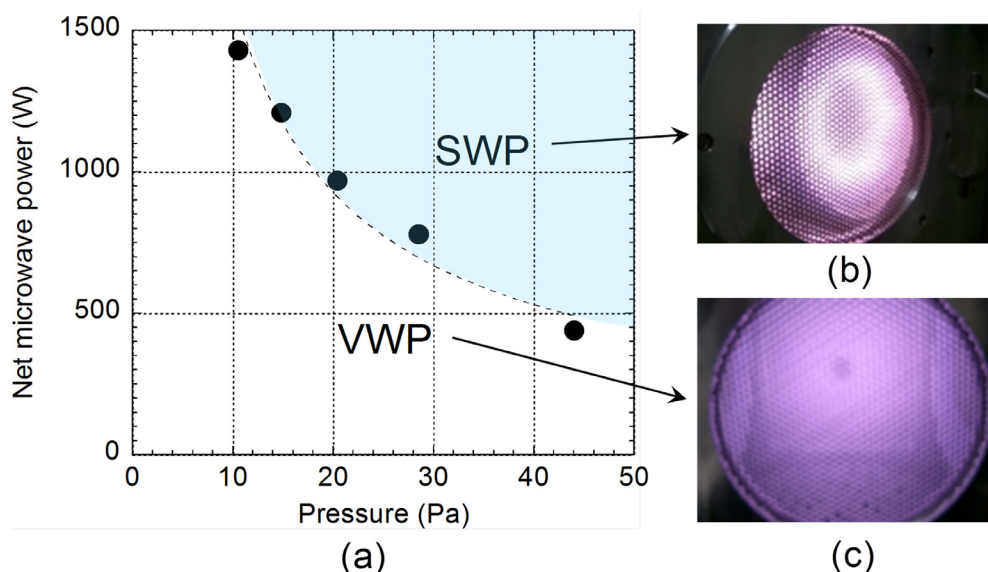


FIG. 7: (a) Relationship between power and pressure for transitions between volume-wave and surface-wave plasma discharges in He gas, with photographs of (b) SWP and (c) VWP

changed to a dark and broad plasma that spread throughout the chamber, which is a typical VWP characteristic, as shown in Fig. 7(c). Because the maximum power available from each magnetron was 1.5 kW, the transition boundary is limited to this maximum power and is observed at a pressure of about 10 Pa.

The plasma parameters, electron density and temperature, of the He gas VWP were also investigated using the double probe technique. The radial distributions of electron densities in the He gas VWP with the single launcher with power of 680 W and double launchers with a power of $380 \text{ W} \times 2$ at 10.5 Pa, and the electron temperature in the He gas VWP with single launcher at 10.5 Pa with power of 680 W are shown in Figs. 8(a) and (b), respectively. Here the probe positions were at $z = 22.5 \text{ cm}$ from the launchers. The density decreased with radial distance; however, the density is fairly broad over a wide area. Because the microwaves penetrated the plasma and might have formed certain electromagnetic wave modes, density was maximum near to the center.²⁶ In the VWP mode, the electron temperature was roughly 6.0 eV, which is comparatively higher than that in the SWP mode.

B. Sterilization Results

To study the sterilization of medical devices, the biological indicators were placed at the center of the discharge chamber on the rotating stage. For this sterilization experiment, we used stable He and air-simulated N_2/O_2 mixture gas SWP at 18 Pa and 1 kW power.

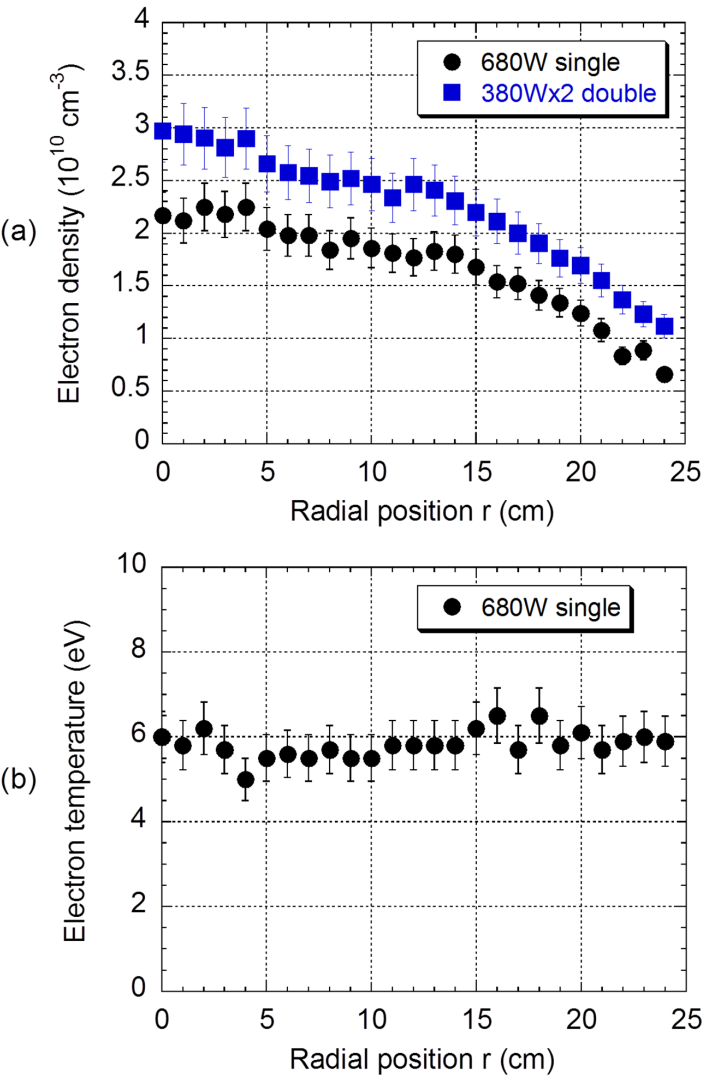


FIG. 8: Radial distributions of (a) electron densities in the He gas VWP with single launcher (at power of 680 W) and double launchers ($380 \text{ W} \times 2$) at 10.5 Pa; and (b) electron temperature in the He gas VWP with single launcher at 10.5 Pa (680 W), respectively

Figure 9 shows the substrate temperature versus the plasma irradiation periods with various on and off cycles. It is obvious that in the 30-sec plasma on and 60-sec off cycle (i.e., 33% duty cycle) the temperature increment was very low compared to other experimental conditions. Additional sterilization experiments were performed with this on/off cycle. With time-modulated SWP at the previously mentioned discharge conditions, the exposed spores were sterilized within 30 min net plasma irradiation and below 65°C .

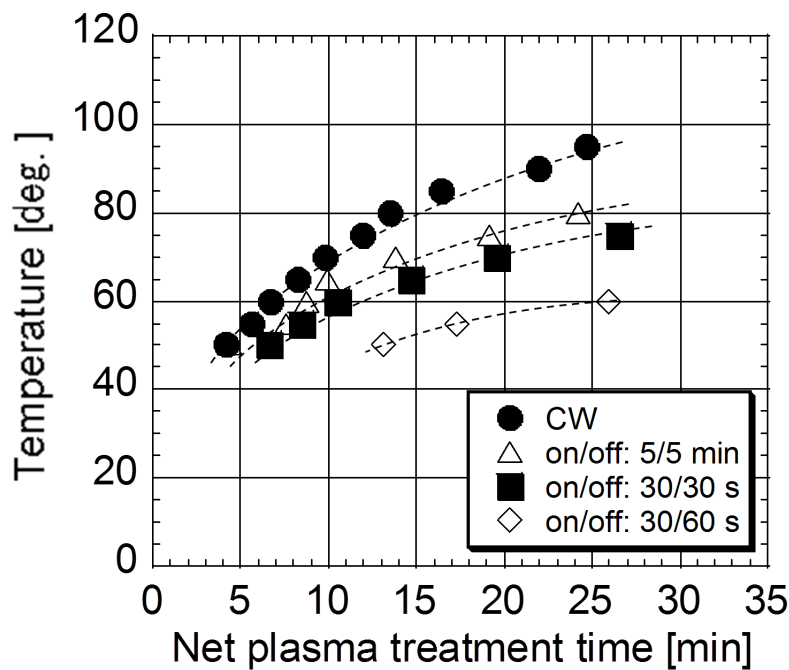


FIG. 9: Stage temperature versus net plasma treatment periods for different on/off cycles

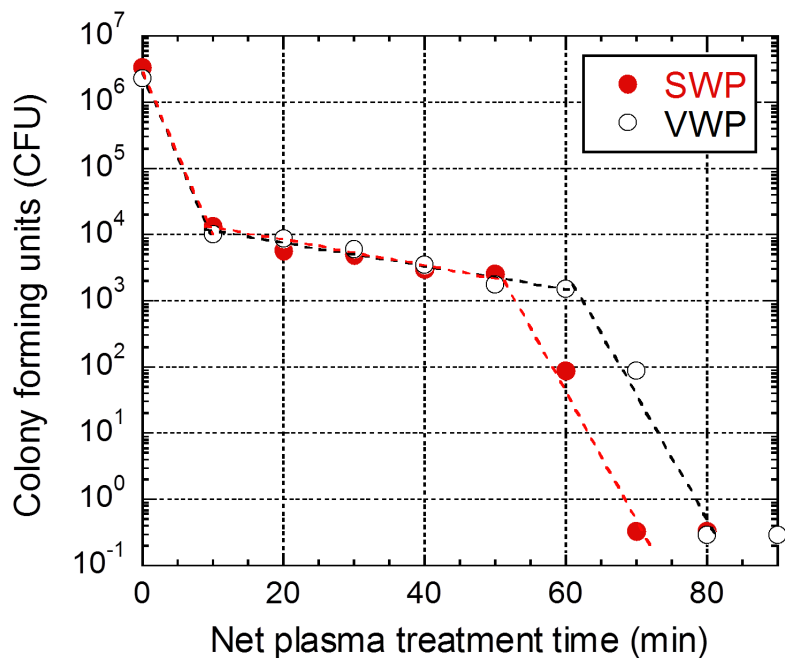


FIG. 10: Survival curve of Tyvek wrapped *G. stearothermophilus* spores treated with (a) SWP and (b) VWP with He plus N₂/O₂ mixture gas, respectively

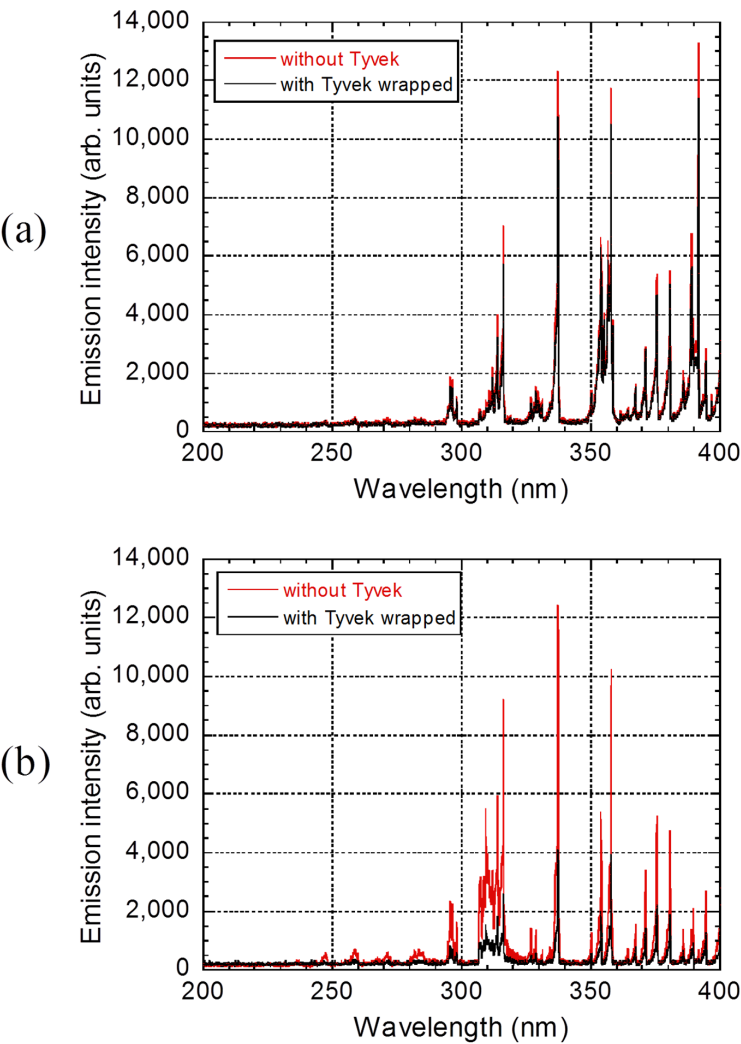


FIG. 11: Optical emission spectra with and without Tyvek wrapping in He plus N₂/O₂ mixture gas; (a) SWP at 18 Pa and 1kW, and (b) VWP at 11 Pa and 1kW

The survival curve, which is a plot of the logarithm of the number of surviving spores as a function of exposure time to the plasma, was plotted for Tyvek wrapped spore samples, and it is shown in Fig. 10. It is interesting to note that the survival curve has a multislope characteristic, which is similar to our previous results.³⁰ Optical emission spectra with and without Tyvek wrapping in He and the N₂/O₂ mixture gas SWP at 18 Pa and 1kW and VWP at 11 Pa and 1kW are shown in Fig. 11, where spectra of UV and other energy emissions that passed through the Tyvek® sheet were observed, , although their intensities were decreased. The strong emission lines at 282.0, 297.7, 313.6, 337.1,

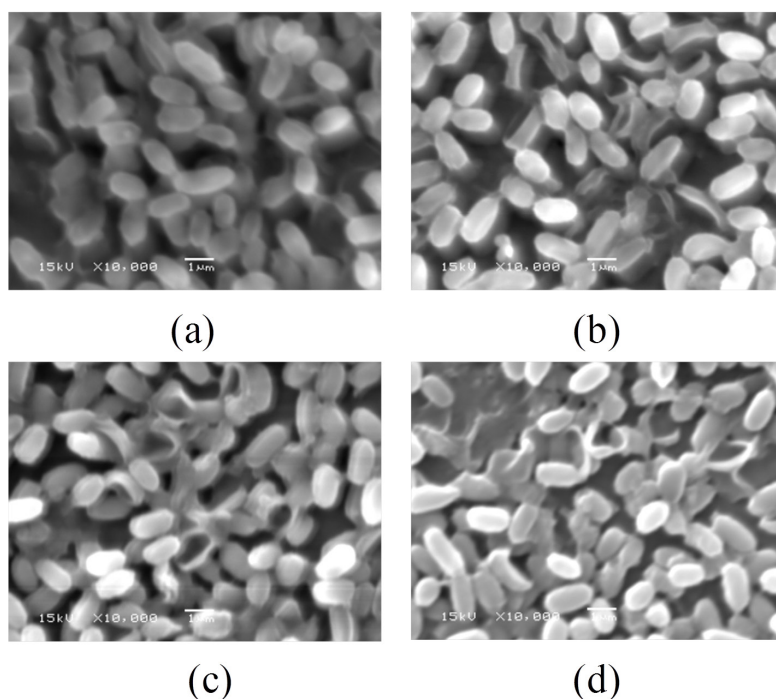


FIG. 12: Scanning electron microscope images of (a) untreated, (b) 10 min, (c) 30 min, and (d) 70 min SWP treated spores. Plasma discharge conditions were He (250 SCCM), N₂ (200 SCCM), and O₂ (50 SCCM) mixture gas with single launcher at 1 kW power.

and 357.7 nm result from the second positive systems ($C^3\Pi_u \rightarrow B^3\Pi_g$) of N₂ molecules.⁹ The UV intensity was not as strong as that of the nitrogen lines. Several UV emissions at 226.9, 237.0, 247.9, and 258.8 nm most likely originated from the NO γ system ($A^2\Sigma^+ \rightarrow X^2\Pi$). Instead of measuring the absolute intensities of these UV, we focused on the biocide species. The UV emissions are well known, and their role in inactivating the spores in addition to the N₂ positive system was very significant in our experiments. Present spectra measurement was limited to 200 nm, which is the minimum observable wavelength of the monochromator. However, wavelengths shorter than 200 nm as well as vacuum UV (VUV) also play a significant role in the sterilization process.^{5,10,12,30}

With the assumption that high electron temperature in the “under-dense” VWP discharges and possibly plasma generation inside the perforated bag will be more effective for inner sterilization of wrapped spores, inactivations in VWP mode were also performed. The stable VWP was generated with He at 250 SCCM, N₂ at 24 SCCM, and O₂ at 10 SCCM in the gas mixture, at 11 Pa and 1 kW incident power. In VWP mode, the glassine wrapped spores (population $\sim 10^3$) were inactivated within 50 min (not shown here) at 65°C, but the Tyvek wrapped spores (population $\sim 10^6$) were inactivated after 80 min at 70°C. The survival curve of Tyvek wrapped spores with VWP treatment is shown in Fig. 10. The similar trend of inactivation was observed in both SWP and

VWP conditions, but the sterilization efficiency in VWP is lower than SWP mode. This may be explained by reduced emission intensity with Tyvek wrapped condition in the VWP mode as compared to SWP mode (Fig. 11), which resulted in lower sterilization efficiency in VWP mode. These results support the assumption that UV/VUV radiation is the main sterilization agent in our experiments. But at the same time, the role of active species in the sterilization efficiency cannot be ruled out in the VWP mode, where the plasma might be produced inside the Tyvek wrapped pouch.

The scanning electron microscopy images of both untreated and SWP treated Tyvek wrapped *G. stearothermophilus* spores were obtained and are shown in Fig. 12. Individual spores exposed to the plasma for 10 min, 30 min, and 70 min revealed no significant changes in the size compared with that of untreated spores, even though the survival curve shown in Fig. 10 indicated that the spores were inactivated after 70 min treatment. Additional experiments are required to understand these seemingly contradictory results and to improve the sterilization characteristics.

IV. CONCLUSION

In conclusion, we investigated a large-volume plasma device to confirm its ability to uniformly sterilize medical devices. The experimental plasma setup consisted of two planar microwave launchers, which were installed face-to-face internally in the vacuum chamber. We observed almost uniform spatial distribution of plasma density in both surface-wave and volume-wave plasmas under various discharge conditions, using single or double launchers in the setup. The electron density measured for the double launchers was approximately twice that of the single launcher, without any microwave interference between two launchers. These experimental results show the feasibility of using the large-volume plasma setup to uniformly sterilize medical equipment with three-dimensional shape. We also confirmed the successful inactivation of both directly exposed and wrapped spore-forming bacteria at temperatures less than 70°C, in considerably short treatment times using time-modulated surface-wave and volume-wave plasmas. The optical emission and morphology of treated spores was studied to understand the sterilization mechanism. Results indicate that UV photons along with additional active species were the main factors contributing to spore sterilization.

ACKNOWLEDGMENTS

This work was partly supported by Grant-in-Aid for Scientific Research (No. 20340161, No. 21110010) from the Japan Society for the Promotion of Science (JSPS) and partly by a grant from the Key Regional Research Promotion program of the Japan Science and Technology Agency (JST). The authors would like to thank Dr. Akihisa Ogino, Mr. Toshiki Mitsui, and Mr. Keigo Ninomiya for their collaboration in the present work.

REFERENCES

1. Moreau S, Moisan M, Tabrizian T, Barbeau J, Pelletier J. Using the flowing afterglow of a plasma to inactivate *Bacillus subtilis* spores: influence of the operating conditions. *J Appl Phys*. 2000 July 15;88(2):1166–74.
2. Moisan M, Barbeau J, Moreau S, Pelletier J, Tabrizian M, Yahia L'H. Low-temperature sterilization using gas plasmas: a review of the experiments and an analysis of the inactivation mechanisms. *Int J Pharm*. 2001;226(1-2):1–21.
3. Moisan M, Barbeau J, Crevier MC, Pelletier J, Philip N, Saoudi B. Plasma sterilization. Methods and mechanisms. *Pure Appl Chem*. 2002;74(3):349–58.
4. Boudam MK, Saoudi B, Moisan M, Ricard A. Characterization of the flowing afterglows of an N₂–O₂ reduced-pressure discharge: setting the operating conditions to achieve a dominant late afterglow and correlating the NO β UV intensity variation with the N and O atom densities. *J Phys D: Appl Phys*. 2007;40(6):1694–711.
5. Pollak J, Moisan M, K'eroack D, Boudam MK. Low-temperature low-damage sterilization based on UV radiation through plasma immersion. *J Phys D: Appl Phys*. 2008;41(13):135212.
6. Nagatsu M, Terashita F, Koide Y. Low-temperature sterilization with surface-wave excited oxygen plasma. *Jpn J Appl Phys*. 2003;42(7B):L856–9.
7. Nagatsu M, Terashita F, Nonaka H, Xu L, Nagata T, Koide Y. Effects of oxygen radicals in low-pressure surface-wave plasma on sterilization. *Appl Phys Lett*. 2005;86(21):211502.
8. Xu L, Terashita F, Nonaka H, Ogino A, Nagata T, Koide Y, Nanko S, Kurawaki I, Nagatsu M. Discharge conditions for CW and pulse-modulated surface-wave plasmas in low-temperature sterilization. *J Phys D: Appl Phys*. 2006;39(1):148–52.
9. Xu L, Nonaka H, Zhou HY, Ogino A, Nagata T, Koide Y, Nanko S, Kurawaki I, Nagatsu M. Characteristics of surface-wave plasma with air-simulated N₂–O₂ gas mixture for low-temperature sterilization. *J Phys D: Appl Phys*. 2007;40(3):803–8.
10. Rossi F, Kylián O, Hasiwa M. Decontamination of surfaces by low pressure plasma discharges. *Plasma Process Polym*. 2006;3(6-7):431–42.
11. Halfmann H, Bibinov N, Wunderlich J, Awakowicz P. A double inductively coupled plasma for sterilization of medical devices. *J Phys D: Appl Phys*. 2007;40(14):4145–54.
12. Halfmann H, Denis B, Bibinov N, Wunderlich J, Awakowicz P. Identification of the most efficient VUV/UV radiation for plasma based inactivation of *Bacillus atrophaeus* spores. *J Phys D: Appl Phys*. 2007;40(19):5907–11.
13. Opretzka J, Benedikt J, Awakowicz P, Wunderlich J, von Keudell A. The role of chemical sputtering during plasma sterilization of *Bacillus atrophaeus*. *J Phys D: Appl Phys*. 2007;40(9):2826–30.
14. Raballand V, Benedikt J, Wunderlich J, von Keudell A. Inactivation of *Bacillus atrophaeus* and of *Aspergillus niger* using beams of argon ions, of oxygen molecules and of oxygen atoms. *J Phys D: Appl Phys*. 2008;41(11):115207.
15. Purevdorj D, Igura N, Ariyada O, Hayakawa I. Effect of feed gas composition of gas discharge plasmas on *Bacillus pumilus* spore mortality. *Lett. Appl. Microbiol*. 2003;37(3):31–4.
16. Hayashi N, Guan W, Tsutsui S, Tomari T, Hanada Y. Sterilization of medical equipment using radicals produced by oxygen/water vapor RF plasma. *Jpn J Appl Phys*. 2006;45(10B):8358–63.
17. Hury S, Vidal DR, Desor F, Pelletier J, Lagarde T. A parametric study of the destruction efficiency of *Bacillus* spores in low pressure oxygen-based plasmas. *Lett Appl Microbiol*.

- 1998;26(6):417–21.
18. Lerouge S, Wertheimer MR, Marchand R, Tabriziani M, Yahia L'H. Effect of gas composition on spore mortality and etching during low-pressure plasma sterilization. *J Biomed Mater Res.* 2000;51(1):128–3.
 19. Moisan M, Boudam K, Carignan D, Kéroack D, Levif P, Barbeau J, Séguin J, Kutasi K, Elmoualij B, Thellin O, Zorzi W. Sterilization/disinfection of medical devices using plasma: the flowing afterglow of the reduced-pressure N₂-O₂ discharge as the inactivating medium. *Eur Phys J Appl Phys.* 2013;63(1):10001–46.
 20. Eto H, Ono Y, Ogino A, Nagatsu M. Low-temperature internal sterilization of medical plastic tubes using a linear dielectric barrier discharge. *Plasma Process Polym.* 2008;5(3):269–74.
 21. Laroussi M, Leipold F. Evaluation of the roles of reactive species, heat, and UV radiation in the inactivation of bacterial cells by air plasmas at atmospheric pressure. *Int J Mass Spectro.* 2004;233(1–3):81–6.
 22. Laroussi M. Low temperature plasma-based sterilization: overview and state-of-the-art. *Plasma Process Polym.* 2005;2(5):391–400.
 23. Huang C, Yu Q, Hsieh F, Duan Y. Bacterial deactivation using a low temperature argon atmospheric plasma brush with oxygen addition. *Plasma Process Polym.* 2007;4(1):77–87.
 24. Ehlbeck J, Schnabel U, Polak M, Winter J, Woedtke T, Brandenburg R, Hagen T, Weltmann K-D. Low temperature atmospheric pressure plasma sources for microbial decontamination. *J Phys D: Appl Phys.* 2011;44(1):013002.
 25. Akitsu T, Ohkawa H, Tsuji M, Kimura H, Kogoma M. Plasma sterilization using glow discharge at atmospheric pressure. *Surf Coat Technol.* 2005;193(1–3):29–34.
 26. Ogino A, Naito K, Terashita F, Nanko S, Nagatsu M. Production of volume wave plasma with internally mounted cylindrical planar microwave launcher and two-dimensional field analysis using finite difference time domain method. *Jpn J Appl Phys.* 2005;44(11):L352–4.
 27. Nagatsu M, Naito K, Ogino A, Ninomiya K, Nanko S. Characteristics of surface-wave and volume-wave plasmas produced with internally mounted large-area planar microwave launcher. *Appl Phys Lett.* 2005;87(16):161501.
 28. Nagatsu M, Naito K, Ogino A, Nanko S. Production of large-area surface-wave plasmas with an internally mounted planar cylindrical launcher. *Plasma Sources Sci Technol.* 2006;15(1):37–41.
 29. Fleisch T, Kabouzi Y, Moisan M, Pollak J, Castañeros-Martínez E, Nowakowska H, Zakrzewski Z. Designing an efficient microwave-plasma source, independent of operating conditions, at atmospheric pressure. *Plasma Sources Sci Technol.* 2007;16(1):173–82.
 30. Singh M K, Ogino A, Nagatsu M. Inactivation factors of spore-forming bacteria using low-pressure microwave plasmas in an N₂ and O₂ gas mixture. *New J Phys.* 2009;11(11):115027.

